Explanation for the smoothness of the phase in molecular high-order harmonic generation

C. C. Chirilă and M. Lein
Institute of Physics, University of Kassel, Heinrich-Plett-Straße 40, 34132 Kassel, Germany
and Centre for Quantum Engineering and Space-Time Research (QUEST) and Institut für Theoretische Physik, Leibniz Universität Hannover, Appelstraße 2, 30167 Hannover, Germany
(Received 18 August 2008; revised manuscript received 20 May 2009; published 9 July 2009)

We analyze the orientation dependence of harmonic amplitudes and phases from laser driven H_2^+. We use the Lewenstein model, with and without employing the saddle-point approximation for the summation over electron momenta. This means that the direction of the electron motion is not necessarily restricted to the laser polarization axis in contrast to previous implementations. The model predicts smooth phase jumps by almost π in the orientation dependence. This demonstrates that the smoothness can be explained without Coulomb effects, but these may be relevant for the size of the phase jumps observed in recent experiments.

DOI: 10.1103/PhysRevA.80.013405 PACS number(s): 33.80.Rv, 42.65.Ky

I. INTRODUCTION

High-order harmonic generation (HHG) from atoms in strong laser fields is a well-known process [1,2], which has been widely studied both theoretically and experimentally in the past two decades. It is the conversion of many infrared or visible laser photons into one high-frequency photon in the extreme ultraviolet (xuv) range. In the last years, the interest in molecular gases instead of atomic gases as generating medium has grown strongly. One reason is that molecules have more degrees of freedom, providing additional "control knobs" for optimizing the emitted harmonics. The use of the rotational degree of freedom, for example, is facilitated by the recently developed experimental techniques [3] to control the alignment of molecules, before the driving laser pulse generates harmonics [4,5]. Another reason is that HHG can be a tool to observe molecular structure and dynamics [6–10].

Early insights into the physical mechanism behind harmonic generation can be found in [11]. The physical picture of the harmonic-generation process is summarized by the "simple-man's model" also known as the "three-step model," proposed in [12] and successfully confirmed by later studies [13]. The model describes the microscopic response only. For the macroscopic response of the medium (not discussed here), propagation effects [14] should be accounted for as well. The simple-man's model describes HHG as consisting of three steps: (1) the atom or molecule is tunnel ionized by the laser field; (2) the created electronic wave packet is subsequently accelerated by the laser field and driven back to the ion, and (3) the wave packet upon its return may recombine to the initial ground state. The kinetic energy E_{kin} acquired by the active electron during step (2) is released in the form of an attosecond burst of xuv light with photon energy $\hbar\omega = E_{kin} + I_p$, where I_p is the ionization potential. The process repeats itself every half optical cycle, thus leading to the creation of a train of attosecond pulses [15].

In recent experiments on CO_2 [16–18], it has been achieved to measure not only the amplitudes of the harmonics in molecular HHG, but also their phases. When the dependence of the phase on the molecular orientation is studied for fixed harmonic frequency, one finds a smooth and rapid variation around the orientation angle at which the amplitude is minimal. The size of this phase jump is around π or smaller than π [16,17]. A similar phase jump is observed in the frequency dependence for fixed alignment [18]. The minimum of the harmonic amplitudes at a certain orientation angle is a signature of the structure and orientation of the molecule. For simple molecules (e.g., H_2^+), this minimum can be understood as being due to the two-center interference phenomenon [19], while for more complex molecules (e.g., CO_2) additional effects such as various ionization channels may have to be taken into account [20].

The phase is an essential ingredient to recover the molecular orbital symmetry in the tomographic reconstruction procedure [6]. Also, it allows for the reconstruction of the time profile of attosecond pulses [18]. The complete temporal characterization of the attosecond emission is relevant for experiments which would make use of the attosecond pulse train to extend quantum control to the xuv and attosecond regime.

A suitable theoretical tool to analyze the harmonic phase is the quantum-mechanical version of the three-step model, known as the strong-field approximation (SFA) or the Lewenstein model [21]. This model involves a three-dimensional (3D) integration over all possible momenta of the active electron between ionization and recombination. In the usual implementation, the integrand is evaluated by using the saddle-point approximation (SPA) [13,21], i.e., the integrand is replaced by an expression that accounts only for the most contributing momentum. This SPA procedure is similar to the selection of the most contributing (classical) trajectory in the Feynman path integral formalism. A characteristic feature of the saddle-point SFA (SP-SFA) is that the continuum electron always moves parallel to the laser polarization. The other major approximation in this model is that it does not incorporate the effect of the Coulombic atomic or molecular binding potential. This implies that the recombination step is described by a transition matrix element with a plane wave for the continuum state. In a simple picture, the orientation dependence in HHG is mainly determined by this matrix element with the plane-wave momentum along the laser field and its value fixed by the energy conservation as explained in step (3). This picture predicts sudden phase jumps by π (see

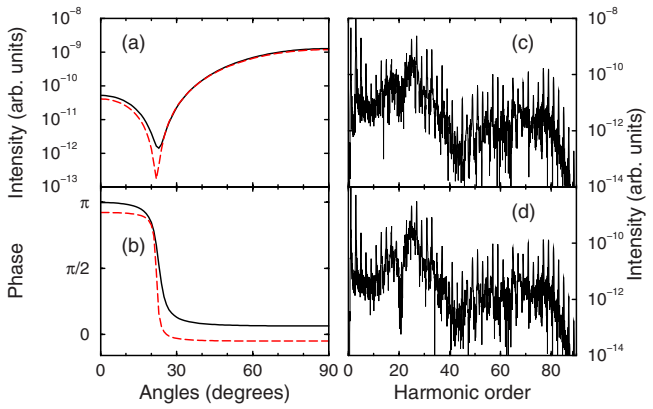

FIG. 1. (Color online) Left panels—comparison of the EX-SFA (black, continuous curves) and the SP-SFA (red, dashed curves) calculations for the 43rd harmonic: (a) the harmonic intensity and (b) the harmonic phase as a function of the molecular orientation angle. Right panels—harmonic spectrum for the orientation $\theta=20°$: (c) SP-SFA result and (d) the EX-SFA result.

Fig. 1 of [22]). Sharp jumps are also produced by versions of the SFA [23] where an additional saddle-point approximation is applied to the temporal Fourier transformation. In recent calculations of the recombination matrix elements, the plane waves that describe the returning electron in the SFA have been replaced by two-center continuum wave functions [22]. The predicted phase jump is smooth and differs from π. Therefore, Coulomb effects have been invoked as a possible explanation of the measured data in [18].

The purpose of this work is to investigate the full prediction power of the plane-wave SFA model for the harmonic emission, without using the SPA. Our main focus is the harmonic phases for both the harmonics polarized along and perpendicular the direction of the laser electric field. Our calculations are therefore also relevant for the interpretation of the experimental data concerning the polarization of the harmonics from CO_2 [24]. In the latter work it has been pointed out that the SP-SFA model breaks down at orientation angles of 0° and 90° of CO_2 relative to the laser field due to the nodal planes of the π_g highest-occupied molecular orbital in the CO_2 molecule. For symmetry reasons, SP-SFA wrongly predicts no harmonic emission at these angles. We present here the predictions of the exact SFA model (EX-SFA), which includes all electron momenta between ionization and recombination. This implies that the momentum of the returning electron need not be strictly parallel to the laser polarization. We compare EX-SFA to the results obtained from the SP-SFA and to the Coulomb-corrected results of [22]. We demonstrate that the smoothness of the phase jump is explained within the plane-wave model and does not require Coulomb effects. Taking Coulomb effects into account by using two-center continuum functions [22] within the present SFA formalism is desirable but causes numerical problems due to the normalization factor being singular at zero momentum. The singularity could be avoided by using the saddle-point approximation for the return time [23]. Atomic units are used throughout this work, unless otherwise specified.

II. THEORY

We consider the H_2^+ molecular ion, at fixed internuclear separation $R=2$ a.u. interacting with linearly polarized laser pulses. We work in the length-gauge version of the dipole approximation, i.e., the Hamiltonian of the laser-field-driven system reads $H(t)=H_0+\mathbf{E}(t)\cdot\mathbf{r}$, where H_0 is the field-free Hamiltonian of H_2^+, $\mathbf{E}(t)$ is the electric field of the laser pulse, and $\mathbf{r}$ is the electron coordinate. Instead of the time-dependent dipole moment, we calculate the time-dependent dipole momentum, since for simple molecules this approach (the velocity form) was shown to give more accurate results within SFA. To obtain the harmonic spectrum, one has to take the modulus squared Fourier transform of the dipole acceleration. The latter is calculated as the time derivative of the dipole momentum. In the SFA model, the expression for the dipole momentum reads:

$$\mathbf{P}_{\rm dip}(t) = -i\int_0^t dt' \int d^3\mathbf{p}\, \mathbf{v}_{\rm rec}^*(\mathbf{p}+\mathbf{A}(t)) \times \exp[-iS(\mathbf{p},t',t)]d_{\rm ion}(\mathbf{p}+\mathbf{A}(t'),t'), \quad (1)$$

where $\mathbf{A}(t)=-\int^t dt'\mathbf{E}(t')$. The quantities $\mathbf{v}_{\rm rec}$ and $d_{\rm ion}$ are the recombination and the ionization matrix elements, respectively. The ionization matrix element describes the transition from the initial bound state Ψ_0 to a continuum state (here approximated by a plane wave) via the interaction with the external electric field, $d_{\rm ion}(\mathbf{p},t)=(2\pi)^{-3/2}\langle\exp(i\mathbf{p}\cdot\mathbf{r})|E(t)z|\Psi_0\rangle$. The recombination matrix element describes the transition from a continuum state to the initial state: $\mathbf{v}_{\rm rec}(\mathbf{p})=(2\pi)^{-3/2}\langle\exp(i\mathbf{p}\cdot\mathbf{r})|-\hat{\mathbf{p}}|\Psi_0\rangle$. Here, z is the coordinate along the laser polarization direction, and $\hat{\mathbf{p}}$ is the momentum operator of the electron. For this work, we consider the gerade σ_g ground state of H_2^+ and the ungerade σ_u 1st excited state of a modified H_2^+ system with nuclear charges chosen to yield the same ionization potential as the σ_g state. Each state is approximated by a linear combination of two atomic orbitals (LCAO). The atomic orbitals are hydrogenic $1s$ wave functions with an exponential decay corresponding to an atomic nuclear charge $Z_{\rm AO}=1.11$ for the σ_g state. This nuclear charge value minimizes the LCAO ground-state energy expectation value. For the σ_u state we use $Z_{\rm AO}=1.49$. This value follows from requiring that the minimization of the σ_u energy expectation value gives the same ionization potential as the σ_g state. The total quantum mechanical phase accumulated by the electron between the ionization time t' and the recombination time t is given by the semiclassical action $S(\mathbf{p},t,t')=(t-t')I_{\rm p}+\int_{t'}^t dt''[\mathbf{p}+\mathbf{A}(t'')]^2/2$, with $I_{\rm p}=1.1$ a.u. being the ionization potential of the initial bound state Ψ_0. In the usual SP-SFA, the integration in Eq. (1) over the electron momenta $\mathbf{p}$ is approximated by the saddle-point method, with the saddle-point momentum $\mathbf{p}_s(t,t')=-\int_{t'}^t dt''\mathbf{A}(t'')/(t-t')$ [21]. The use of only one momentum value can be interpreted as taking into account only the most contributing electron trajectory for every pair of times (t,t'), while neglecting the rest. In our work, we calculated fully the expression in Eq. (1), without resorting to the SPA for the integration over momenta. This means that apart from the two-dimensional integration over the ion-

ization and the recombination times required, one has to add an extra three-dimensional integration over all possible electron momenta to obtain the HHG spectrum. We have accomplished this formidable numerical task with the help of the generalized Feynman identity [25] and of a specifically tailored numerical quadrature method [26]. The Feynman identity is used to analytically integrate over the orientation of the electron momenta, thus reducing the integral to a two-dimensional one (keeping in mind that the use of the Feynman identity introduces one additional integration). For one variable, the integration range is finite and the integrand is very smooth, while for the other variable the integration is of the type of a Fourier transformation over the real semi-axis. The latter is done numerically with the help of the method described in [26].

To emphasize the drawback of the SP-SFA, we inspect the expression of the ionization matrix amplitude, remembering that $\mathbf{p}_s$ is oriented along the laser polarization axis. If Ψ_0 possesses mirror antisymmetry and the field is parallel to the nodal plane of Ψ_0, then d_{ion} is identically zero and no prediction for the harmonic spectrum is possible. Moreover, for any orbital orientation within the velocity form of the SP-SFA, there are no predictions for the harmonics polarized perpendicular to the laser field. This problem arises because the momentum operator in the expression for $\mathbf{v}_{\mathrm{rec}}$ can be taken to act on the plane wave, leading to $\mathbf{v}_{\mathrm{rec}}(\mathbf{p}_s)\|z$. These shortcomings are not present when the full calculation is performed according to Eq. (1). On the other hand, the SPA significantly reduces the computational effort, while providing in many cases an acceptable level of accuracy (see below). The figures show results for harmonics polarized parallel to the field, unless otherwise specified.

III. RESULTS AND DISCUSSION

Figure 1 shows a comparison between the results of the full calculation (EX-SFA) and the SP-SFA for the σ_g ground state. The laser pulse has an intensity of 5×10^{14} W/cm^2 and a central wavelength of 780 nm. The electric field of the laser pulse has a trapezoidal envelope, with 5 optical cycles each for turn on and off and 5 cycles of constant amplitude. In the figure, we analyze the 43rd harmonic in order to compare directly to Fig. 1 in [22]. The phase change across the value of the orientation angle where the amplitude goes through a minimum is smoother in the EX-SFA than in the SP-SFA (in this case as well as in the majority of cases, but not always). The positions of the amplitude minimum are slightly different in the two calculations. The difference with respect to earlier results from the time-dependent Schrödinger equation [19] is related to the fact that we do not include the *ad hoc* correction of the return energy by I_p that was suggested in [19]. An important observation is that the width of the phase jump is larger than the width in Fig. 1 of [22], which was purely due to Coulomb effects. Panels (c) and (d) of Fig. 1 show that the HHG spectra are overall rather similar in the two calculations.

Figure 2 shows the comparison between the EX-SFA and SP-SFA for three different harmonic orders. The 41st, 61st, and the 83rd harmonics are located in the harmonic plateau region, close to cutoff, and shortly after the cutoff at $3.17U_p+I_p=80.5\omega_L$, respectively. (U_p is the ponderomotive potential and ω_L is the laser frequency.) The SPA results are seen to follow roughly the EX-SFA results, except for some angles where the agreement is less satisfactory. For the 41st harmonic, the phase is almost constant, since there is no fully developed minimum in the harmonic amplitude. For the other two harmonics, the phase undergoes a change by approximately π when the amplitude passes through the minimum.

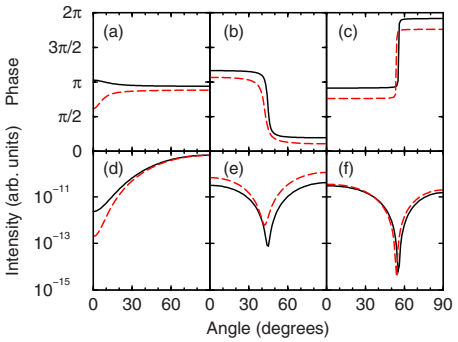

FIG. 2. (Color online) Orientation dependence of harmonic phase and intensity for the H_2^+ σ_g ground state. The EX-SFA results are depicted by continuous, black curves and the SP-SFA results are shown by red, dashed curves. Panels (a) and (d): 41st harmonic. Panels (b) and (e): 61st harmonic. Panels (c) and (f): 83rd harmonic.

In Fig. 3, the initial state is taken to be the σ_u state. Clearly visible here is that the SP-SFA fails near the orientation angle $\theta=90°$, as expected.

We proceed with the analysis of the harmonics polarized perpendicular to the laser field. Figure 4 shows the results for the σ_g state. Compared to the harmonics polarized along the laser polarization direction (see Fig. 2), these harmonics are at least two orders of magnitude lower, and thus mostly negligible. Notice the phase jump by π at the angles 0° and 90° where minima occur in the intensity. A similar picture (not shown here) is found also for the case of the σ_u state. The small yield of the perpendicular component is physically reasonable since we approximate the $\mathbf{H}_2^+$ molecular orbital as an LCAO composed of spherically symmetric atomic orbitals. Note that the experimental observation of nonparallel harmonics relied on aligned CO_2 molecules, for which the highest occupied molecular orbital is composed of nonspherical atomic p orbitals. The nonzero yield predicted by the EX-

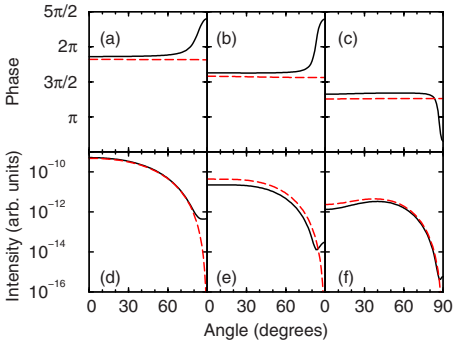

FIG. 3. (Color online) Same as Fig. 2 for the σ_u state.

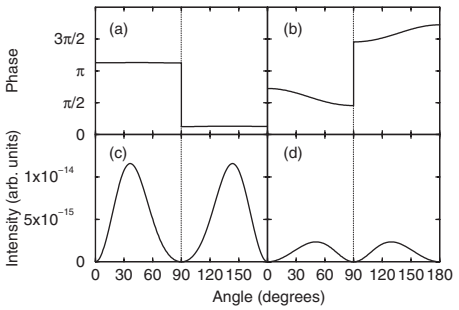

FIG. 4. Orientation dependence for the harmonics polarized perpendicular to the laser field (EX-SFA results for the σ_g state only). Panels (a) and (c) show the 41st harmonic, (b) and (d) the 61st harmonic.

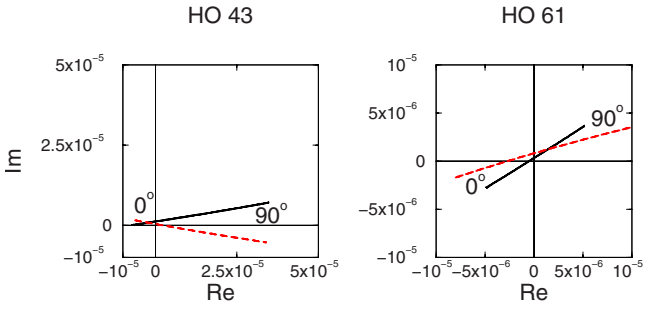

FIG. 5. (Color online) The real and imaginary parts of the complex amplitude for the 43rd (left panel) and 61st (right panel) harmonics, from the EX-SFA (black, continuous curve) and from the SP-SFA (red, dashed curve).

SFA is due to the fact that the electron momenta are not strictly parallel to the laser field. Comparison of Figs. 4(a) and 4(b) with Figs. 2(a) and 2(b) suggests that the variation in the phase for the 61st harmonic is related to the two-center interference although no such structure is visible in the harmonic intensity of the perpendicular component.

The phase jump for a given harmonic can be visualized in a complementary way: Fig. 5 shows the orientation dependence of the complex harmonic amplitude of the 43rd and 61st harmonic for both the SP-SFA and EX-SFA calculations as curves in the complex plane. The points corresponding to 0° and 90° are at the beginning and at the end of each line. The phase jump occurs when the line passes by the origin. The phase difference between the end points of the line is almost equal to π. It is remarkable that the curves are almost straight lines in the complex plane, giving rise to near-π phase jumps.

IV. CONCLUSION

We have analyzed in this paper the predictions of the strong-field approximation, without employing the saddle-point method. This way, the full prediction power of the model can be assessed. The differences with respect to the SP-SFA results are non-negligible. Our EX-SFA approach overcomes the limitations of the SP-SFA and allows to analyze the harmonic phases and amplitudes for all molecular orientation angles and harmonic polarization directions. For a given harmonic order, the orientation dependence of the complex harmonic amplitude is an almost straight line in the complex plane, explaining in an intuitive graphical manner the phase jump close to π. This means that the phase jump by significantly less than π observed in the experiment [18] cannot be explained in the plane-wave SFA model. However, the model does explain the smoothness of the phase jump and it predicts a significantly broader width than Coulomb effects. We conclude that even though Coulomb effects are generally important, they appear to be of minor relevance as far as the description of the width of the phase jump is concerned.

One may expect that propagation effects affect the harmonic phases, especially their absolute values, by macroscopic selection of certain trajectories. The orientation dependence of the phases, however, results mainly from the recombination step at the molecular level and, as we have shown here, from the uncertainty in the recombination momentum due to non-saddle point dynamics. These effects are present independent of the type of electron trajectory. Hence, we expect that propagation effects will not undo the smooth behavior of the phases. However, the short trajectories imply less transverse spatial spreading of the electron wave packets and thus a larger momentum spread for the recombining electron. If propagation effects select the short trajectory, an even smoother phase may therefore be expected.

ACKNOWLEDGMENT

This work was supported by the Deutsche Forschungsgemeinschaft.

[1] A. McPherson *et al.*, J. Opt. Soc. Am. B **4**, 595 (1987).
[2] A. L'Huillier, K. J. Schafer, and K. C. Kulander, J. Phys. B **24**, 3315 (1991).
[3] H. Stapelfeldt and T. Seideman, Rev. Mod. Phys. **75**, 543 (2003).
[4] R. Velotta, N. Hay, M. B. Mason, M. Castillejo, and J. P. Marangos, Phys. Rev. Lett. **87**, 183901 (2001).
[5] J. Itatani, D. Zeidler, J. Levesque, M. Spanner, D. M. Villeneuve, and P. B. Corkum, Phys. Rev. Lett. **94**, 123902 (2005).
[6] J. Itatani *et al.*, Nature (London) **432**, 867 (2004).
[7] T. Kanai, S. Minemoto, and H. Sakai, Nature (London) **435**, 470 (2005).
[8] S. Baker *et al.*, Science **312**, 424 (2006).
[9] N. L. Wagner *et al.*, Proc. Natl. Acad. Sci. U.S.A. **103**, 13279 (2006).
[10] M. Lein, J. Phys. B **40**, R135 (2007).
[11] J. L. Krause, K. J. Schafer, and K. C. Kulander, Phys. Rev. Lett. **68**, 3535 (1992).

[12] P. B. Corkum, Phys. Rev. Lett. **71**, 1994 (1993).
[13] P. Salières *et al.*, Science **292**, 902 (2001).
[14] M. Geissler, G. Tempea, and T. Brabec, Phys. Rev. A **62**, 033817 (2000).
[15] P. M. Paul *et al.*, Science **292**, 1689 (2001).
[16] N. Wagner, X. Zhou, R. Lock, W. Li, A. Wuest, M. Murnane, and H. Kapteyn, Phys. Rev. A **76**, 061403(R) (2007).
[17] X. Zhou, R. Lock, W. Li, N. Wagner, M. M. Murnane, and H. C. Kapteyn, Phys. Rev. Lett. **100**, 073902 (2008).
[18] W. Boutu *et al.*, Nat. Phys. **4**, 545 (2008).
[19] M. Lein, N. Hay, R. Velotta, J. P. Marangos, and P. L. Knight, Phys. Rev. Lett. **88**, 183903 (2002); Phys. Rev. A **66**, 023805 (2002).
[20] O. Smirnova, S. Patchkovskii, Y. Mairesse, N. Dudovich, D. Villeneuve, P. Corkum, and M. Y. Ivanov, Phys. Rev. Lett. **102**, 063601 (2009).
[21] M. Lewenstein, P. Balcou, M. Y. Ivanov, A. LHuillier, and P. B. Corkum, Phys. Rev. A **49**, 2117 (1994).
[22] M. F. Ciappina, C. C. Chirilă, and M. Lein, Phys. Rev. A **75**, 043405 (2007).
[23] E. V. van der Zwan, C. C. Chirilă, and M. Lein, Phys. Rev. A **78**, 033410 (2008).
[24] J. Levesque, Y. Mairesse, N. Dudovich, H. Pepin, J. C. Kieffer, P. B. Corkum, and D. M. Villeneuve, Phys. Rev. Lett. **99**, 243001 (2007).
[25] R. P. Feynman, Phys. Rev. **76**, 769 (1949).
[26] T. Ooura and M. Mori, J. Comput. Appl. Math. **112**, 229 (1999).